Advancing Precision in Spinal Cord Shock Wave Therapy: Design, Development, and Validation of a Real-Time Angle Measurement System for optimized Applicator Alignment

Alexander Plattner

***Abstract*—Spinal cord injury (SCI) is a devastating indication followed by motor and sensory impairments. Current research does not show any non-invasive therapy methods for long-term functional improvement. Extracorporeal shockwave therapy (ESWT) has shown clinical evidence in various musculoskeletal indications due to its regenerative effects. Research in ESWT of the spinal cord following SCI demonstrated preclinical evidence in animal studies. Furthermore, an initial human study was conducted to validate the outcomes of the animal studies, and a larger clinical trial is currently underway, without any feedback systems for the applicator alignment. For spinal cord shockwave therapy, it is important to emit shockwaves in a desired angle to effectively target the spinal cord lesion and therefore maximize the therapeutic outcome. Otherwise, the vertebrae may reflect a significant amount of energy, thereby reducing the arriving energy at the lesion site and hence the therapeutic effect.**

This paper introduces the use of an inertial measurement unit (IMU) to measure the acceleration and angular velocity of the shockwave head. The raw data of the IMU where processed and utilized for the angle estimation using a complementary filter, which effectively mitigates the drawbacks of the accelerometer and gyroscope to precisely estimate the angular displacement of the shockwave head during shockwave emission.

The system showed accurate angle measurement results during the verification with an optical encoder. For pitching, a mean deviation of 1.37° and for rolling, a mean error of 0.34° were achieved. Despite the low absolute errors for pitch and roll, the mean error for yawing is elevated at 7.98°, as the yaw angle estimation relies solely on the gyroscope data. Nevertheless, this inaccuracy can be neglected because the shockwaves are emitted in the same direction irrespective of the yaw angle. The compatibility of the IMU with the high-voltage discharge of the electrohdyraulic shockwave head has been demonstrated. Mean maximum peak values of $0.161\,\mathrm{g}$ for acceleration and $1.654\,\mathrm{s}^{-1}$ for angular velocity were measured. The peaks in the IMU data refer to the emission of shockwaves but does not influence the calculation of the angular displacement due to the robust complementary filter.

This paper successfully implemented an angle measurement system for spinal cord shockwave therapy and demonstrated its resistance to electromagnetic interference from the shockwave head. Further research needs to be conducted to minimize the size of the shockwave applicator, transform the prototype into a commercial product and proof the safety and efficacy within clinical trials.

***Index Terms*—Extracorporeal shockwave therapy, Spinal cord injury, Inertial Measurement Unit**

A. Plattner is with the Department of Medical and Health Technologies, MCI, Innsbruck, Austria, e-mail: a.plattner@mci4me.at.

Manuscript received July 31, 2024.

I. Introduction

ACCORDING to the World Health Organization (WHO) every year between $250\,000$ and $500\,000$ people suffer a spinal cord injury (SCI) worldwide due to reasons like traffic accidents, falls and violence [1]. Currently, there is no effective regenerative treatment for SCI available which addresses the neurological anomalies [2]. Current procedures involve immediate resuscitation, physical therapy and palliative care of secondary injuries like pressure ulcers, spasticity, cardiovascular and pulmonary complications and many more [2], [3]. Stem cell therapy has achieved clinical relevance in spinal cord treatment due to the promising results, but the transplanted cells do not survive over a longer period of time [2]. Therefore there is the clinical need for a regenerative treatment method for functional or neurological impairments following traumatic SCI.

Shockwaves have been utilized in medicine since 1980 for the purpose of destructing kidney stones [4]. Due to a random observation of iliac bone thickening in x-rays after lithotripsy, the idea emerged to use shockwaves not only in a destructive manner but also perform research of its regenerative effects [5]. Due to the regenerative effect of shockwaves, different application fields arose. Extracorporeal shockwave therapy (ESWT) shows clinical evidence in musculoskeletal disorders such as pseudoarthrosis, achilles tendinopathy, plantar fasciitis, calcified shoulder, tennis elbow, etc. [6].

The systematic review paper [7] illustrates preclinical evidence based on animal studies that the application of shockwaves to the spinal cord yields improved locomotor recovery and regenerative effects to the neural tissue following SCI. Graber et al. [8] conducted the first in-human clinical trial where five patients underwent ESWT after SCI due to aortic dissection or surgery. Due to the small number of patients included in this clinical trial, Leister et al. [9] initiated a clinical trial enrolling 82 patients, who have recently experienced traumatic SCI for the initial phase. The current procedure in ESWT of the spinal cord involves emitting shockwaves at the level of the lesion and five segments above and below. The shockwave head is held in an approximated angle of 45° paravertebral from both sides [9].

However, a critical challenge arises due to the presence of the vertebral arch with its transverse and spinous processes which is boney tissue and therefore reflects the shockwaves,

hence reducing the arriving energy at the spinal cord. According to Reinhardt et al. [10], who examined the attenuation of the positive peak pressure of shockwaves by the skull, found that the skull bone dampens shockwaves by $84\,\%$. Therefore, it is important to apply the shockwaves to the spinal cord at the correct angle to ensure that no bony structures attenuate the pressure of the shockwave, thereby preserving the therapeutic outcome.

To effectively target the spinal cord with shockwaves, the shockwave applicator must be tilted along the longitudinal and transversal axes by a predefined angle. These angles vary along the entire length of the spinal cord due to the diverse shapes of the vertebral arches and their processes. Currently the tilting of the applicator is approximated using anatomical landmarks, and no precise angle measurement is conducted during the treatment. This reliance on estimations introduces a degree of uncertainty and may lead to suboptimal treatment outcomes. Therefore, there is a pressing need to develop a method that ensures accurate and reproducible tilting of the shockwave applicator. This will not only enhance the effectiveness of the treatment but also contribute to the overall advancement of SCI therapies.

The emerging area of ESWT for neurological disorders such as Alzheimer's disease uses a real-time navigation system based on an infrared camera to precisely guide the shockwave applicator to the targeted area, ensuring effective treatment [11], [12].

The purpose of this paper is to develop a precise and reliable system for real-time angle measurement and adjustment of a shockwave applicator during SCI treatments. The goal is to enhance the accuracy of shockwave delivery, thereby optimizing the therapeutic impact and potential regenerative effects on the spinal cord. The leading question will be, how the development and implementation of a real time angle measurement system can contribute to the precise alignment of shockwave applicators during SCI treatment.

II. Methods

A. System

The system needs to be capable of accurately estimating the angle displacement of the shockwave head in all three axes. Additionally, the angle should be visually displayed. When the shockwave head is held in the desired position, light-emitting diodes (LED) should indicate it. Via a button it should be possible to reset the orientation of the shockwave head, allowing the system to set the null reference which aligns with the spinal cord.

To estimate the three-dimensional angle displacement of the shockwave head, the Inertial Measurement Unit (IMU) MPU-9250 from Invensense was used. The computational operations are performed by the NUCLEO-L432KC microcontroller from STMicroelectronics. The requirements for the visual display are covered by an OLED display and two RGB LEDs. The OLED display visualizes the current angle displacement in the longitudinal and transversal axis. One LED indicates the correct angle displacement along the longitudinal axis, while the other LED indicates it along the transversal axis. Resistors

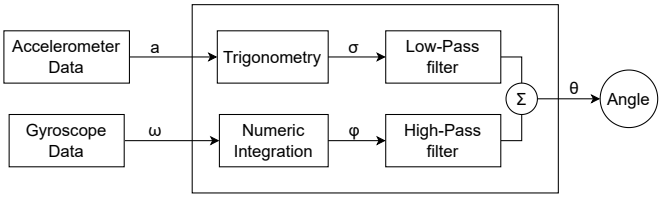

Figure 1. Angle estimation algorithm using a complementary filter [13].

are connected in series with the LEDs to limit the current and therefore protect the LEDs from damage. A button is installed to reset the orientation of the shockwave applicator. The system is powered by a $5\,\mathrm{V}$ USB power supply.

1) Gyroscope calibration: During the initialization phase of the system, the gyroscope was calibrated. Therefore, the offset was determined by reading the raw gyroscope data 1500 times and subsequently calculating the arithmetic mean. The acquired mean offset value of the gyroscope was then subtracted from the read gyroscope data during angle estimation.

2) Angle Estimation Algorithm: The angle was estimated by the accelerometer and gyroscope of the IMU. The drawback of the accelerometer lies in its susceptibility to external forces, while the gyroscope suffers from constant drift. Therefore, sensor fusion was employed to mitigate the drawbacks of both, resulting in a reliable angle estimation. This can be achieved by implementing a complementary filter [13].

The complementary filter was structured as follows. The angle calculated based on the angular velocity ω by integration over time was passed through a high-pass filter. This filters out the drift of the gyroscope. The angle displacement φ based on the angular velocity ω can be calculated accordingly:

$$\varphi = \int \omega dt \tag{1}$$

The angle obtained by the sensor value of the accelerometer was passed through a low-pass filter, improving the robustness of the angle calculation against external impacts. The angular deviation σ based on the acceleration in all three axis a_x, a_y and a_z can be determined in the following way:

$$\sigma_x = \arctan \frac{a_y}{a_z} \tag{2}$$

$$\sigma_y = \arctan \frac{a_x}{a_z} \tag{3}$$

The final angle value was gained via the summation of the two filter outputs. The block diagram is shown in Figure 1. The formula of the complementary filter is depicted as follows [13]:

$$\theta = \alpha \cdot (\theta + \omega \cdot dt) + (1 - \alpha) \cdot \sigma \tag{4}$$

θ represents the filtered angle, which depends on the previous result of the equation, ω is the angular velocity measured from the gyroscope, σ is the acquired angle from the acceleration of the sensor, dt denotes the time interval between two angle estimations, which was set according to the Equation 5 and α represents the filter coefficient. The filter coefficient

determines the weighting of the accelerometer and gyroscope in the calculation of the angle displacement. To obtain reliable and linear outcome of the angle, the summation of α and $1-\alpha$ needs to be one [14]. In this system, α was set to 0.98. This indicates that the gyroscope was weighted with $98\,\%$, while the accelerometer contributes $2\,\%$ to the final angle value.

The Equation 4 was used for the calculation of the pitching (x-axis) and rolling (y-axis) of the shockwave head. The yawing (z-axis) was determined only from the gyroscope data according to Equation 1 because the accelerometer does not yield reliable results for yawing. For yawing an additional magnetometer needs to be implemented which was not integrated into this system.

An important variable for calculating accurate angle values is the time interval. Therefore, a timer interrupt of the microcontroller was used to precisely execute the calculation of the angles in a specific time interval. The timer interrupt interval can be calculated as follows:

$$dt = \frac{(PSC+1)\cdot(ARR+1)}{f_{CLK}} \tag{5}$$

dt denotes the time interval, PSC represents the prescaler of the timer, ARR indicates the auto-reload register and f_{CLK} stands for the clock frequency of the microcontroller. According to the datasheet of the development board NUCLEO-L432KC the clock frequency is $32\,\mathrm{MHz}$. Consequently, the configuration of the timer interrupt yields a time interval of $4\,\mathrm{ms}$.

3) Reset Orientation: The feature of resetting the orientation is important to align the orientation of the shockwave head with the spine of the patient. To achieve this, a button was implemented into the system which triggers an external interrupt. The interrupt routine temporarily sets the angle measurement on hold and stores the current angle displacement. Once buffered, the angle estimation continues and the stored angle value is subtracted from the subsequent angle measurement results to determine the angle relative to the obtained orientation.

B. Prototype

For the evaluation of the system, the components were soldered on a custom-made printed circuit board (PCB), which was developed with the software „Altium Designer" (Altium Ltd., San Diego, California). Furthermore, a housing was constructed for the cardiac shockwave probe 0200 (CSP0200, HeaRT Regeneration Technologies GmbH, Innsbruck, Austria), where the bottom shell of the housing was extended to place the PCB inside the housing.

Figure 2. Final prototype mounted on the CSP0200 applicator with the PCB fixed with a screw inside the housing.

C. Method for Angle Verification

To verify the accuracy and the precision of the angle estimated by the complementary filter, an optical encoder was utilized. To perform the measurement, the prototype and the disc of the encoder has to be linked together via a shaft. Therefore, the housing of the prototype needs to be extended to allow the shaft to be fixed to it. The extension features a hole where a metal shaft can be inserted. Additionally, the shaft gets tightened by two grub screws placed $90°$ to each other. The other end of the metal shaft was inserted into the disc of the encoder and affixed by the internal screw. Consequently, the prototype and the encoder were linked together and proper tightening avoid that the encoder turns without the prototype turning and vice versa. The extension must be added at three surfaces of the housing in such a way, that the verification of the angle measurement can be performed for each axis.

III. Results

A. System Prototype

The size of the PCB of the final prototype is $36 \times 52\,\mathrm{mm}$, which is placed in the adapted housing of the shockwave applicator. An illustration of the final prototype, affixed on the shockwave applicator CSP0200, can be seen in Figure 2.

B. Angle Measurement Verification

The measurement was executed as follows: The prototype was aligned to $0°$ and the angle of the encoder was reset. Then the prototype was rotated from 0 to $90°$ with a step size of $10°$ and the calculated angle of the prototype was recorded at each step. The measurement was repeated five times to gain a mean value and a standard deviation. By conducting multiple measurements of the same variable, systematic and random errors can be mitigated. This entire process was carried out independently for all three axes: pitch, roll and yaw. The results of the measurement can be seen in Table I. The peaks in the data correspond to the timepoints of the shockwave emission. For pitching, a mean absolute deviation of $1.37°$ was obtained, corresponding to a mean relative deviation of $2.81\,\%$. For rolling, the absolute error is $0.34°$, which corresponds to $0.76\,\%$.

C. Compatibility Test

The compatibility test aimed to demonstrate that the prototype, with its electronic components, is capable of measuring and calculating the angle displacement of the shockwave head during shockwave emission. For this purpose, the NRG-H device (HeaRT Regeneration Technologies GmbH, Innsbruck, Austria) was employed as the high voltage supply, and the CSP0200 applicator was used for shockwave emission.

Table I
MEASUREMENT RESULTS OF THE ANGLE VERIFICATION.

encoder / °	pitch / ° Mean (SD)	roll / ° Mean (SD)	yaw / ° Mean (SD)
0	0.00 (0.00)	0.00 (0.00)	0.00 (0.00)
10	9.87 (0.44)	10.12 (0.53)	9.34 (0.77)
20	20.64 (0.65)	19.82 (0.33)	17.58 (0.80)
30	31.08 (0.57)	29.85 (0.17)	25.86 (0.90)
40	41.56 (0.29)	39.78 (0.59)	34.14 (0.24)
50	51.70 (0.71)	49.31 (0.54)	41.85 (0.76)
60	61.78 (0.79)	59.60 (1.62)	50.01 (0.69)
70	71.94 (0.81)	69.49 (1.15)	58.15 (0.62)
80	82.28 (0.92)	79.54 (0.91)	66.26 (0.71)
90	91.23 (0.84)	90.33 (0.87)	74.98 (0.63)

In the beginning, the compatibility test was conducted without any shielding of the prototype. This unshielded setup led to interference in the timing of the microcontroller, resulting in inaccurate angle measurement results. Consequently, the test was continued with the prototype shielded by an aluminum foil connected to ground, which reduced the electromagnetic interference.

During the test, the measurement results from the accelerometer and gyroscope, as well as the calculation of the angle displacement depending on the distance between the shockwave head and the prototype, were examined. The IMU data were obtained at two different distances between the prototype and the shockwave applicator: once at $0\,\mathrm{cm}$ and once at $20\,\mathrm{cm}$. Shockwaves were emitted at a frequency of $4\,\mathrm{Hz}$ and an energy flux density of $0.35\,\mathrm{mJ\,mm^{-2}}$. For the evaluation, data from the accelerometer and gyroscope were recorded for 20 shockwaves to assess if the peaks in the datasets accumulated over time. For the evaluation of the angle data, 10 shockwaves were included. The IMU data during shockwave emission are shown in Figure 3 and 4. The mean peak values for acceleration and angular velocity in all three axes depending on the distance between the shockwave head and the prototype are depicted in Table II.

Table II
MEAN PEAK VALUES DURING COMPATIBILITY TEST, VALUES GIVEN IN THE FOLLOWING FORMAT: MEAN (SD).

d / cm	0	20
a_x / g	0.062 (0.018)	0.052 (0.112)
a_y / g	0.043 (0.027)	0.036 (0.106)
a_z / g	0.161 (0.193)	0.078 (0.208)
ω_x / s^{-1}	0.534 (0.382)	0.289 (0.224)
ω_y / s^{-1}	1.654 (1.040)	0.456 (0.378)
ω_z / s^{-1}	1.275 (0.355)	0.242 (0.174)

IV. DISCUSSION

In this paper, the effective implementation of an accurate angle measurement system inside a shockwave head was demonstrated. To obtain an accurate angle displacement of the shockwave head, an IMU was used to gather the raw data, and a subsequent sensor fusion was performed. To integrate the real-time angle measurement system inside a shockwave head, a PCB was designed, and the bottom shell of the CSP0200 applicator was extended to assemble the PCB within the housing.

The complementary filter has been used as a sensor fusion algorithm to calculate the angle displacement of the shockwave head through sensor fusion of the accelerometer and gyroscope data. Gui et al. [13] compared the complementary filter with the Kalman filter, highlighting these two as the most prominent methods for sensor fusion. Both filters demonstrated accurate results in their examination. However, the complementary filter is beneficial in terms of computational power and workload because it requires the tuning of only one filter parameter, the weighting α. In comparison, the Kalman filter requires three filter coefficients, which takes more time to determine the optimal filter coefficients for the specific application [13].

To verify the accuracy and precision of the angle measurement, the utilization of the encoder has shown feasibility. For the pitching and rolling of the shockwave head, high accuracy and precision were achieved. The standard deviation between the measurement rounds is low, indicating high precision. The

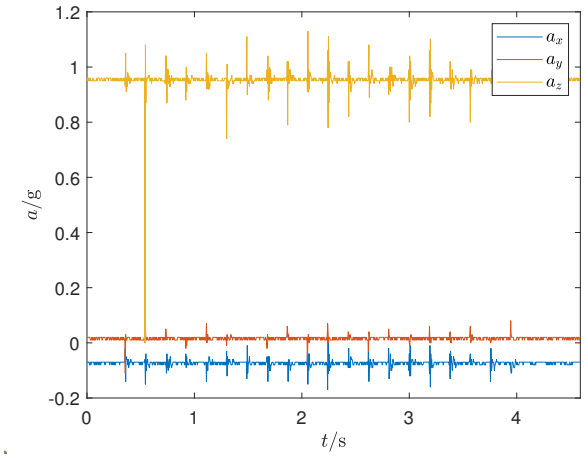

Figure 3. Accelerometer data at $0\,\mathrm{cm}$ distance between the shockwave head and the prototype during the compatibility test.

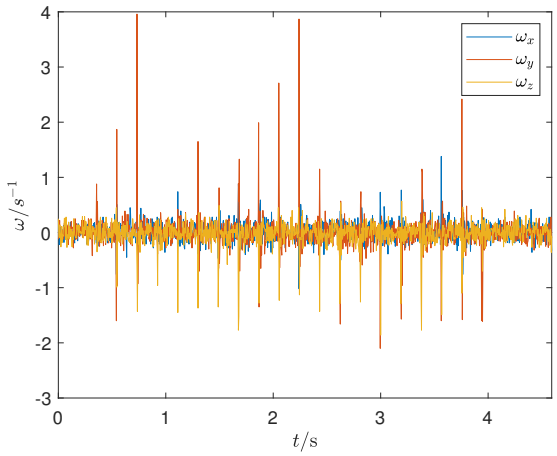

Figure 4. Gyroscope data at $0\,\mathrm{cm}$ distance between the shockwave head and the prototype during the compatibility test.

mean deviation between the measured value and true value is also low, indicating high accuracy.

Although the absolute and relative errors for pitching and rolling are low, the error for yawing is elevated at $7.98°$ which is equivalent to $14.54\,\%$ relative error. As already mentioned, the yaw angle, equivalent to the angular displacement around the z-axis, is solely obtained from the gyroscope. The accelerometer is not considered in estimating the yaw angle because the acceleration does not change during yawing, as the gravity vector is parallel to the z-axis. In contrast, the gravity vector is perpendicular to the x-axis and y-axis for pitch and roll, allowing the accelerometer to measure changes. To gain reliable results for the yaw angle, a magnetometer has to be integrated into the system. Then the yaw angle can be calculated based on the change in the Earth's magnetic field [15].

For the spinal cord shockwave therapy, the longitudinal and transversal displacement of the shockwave head are important. The rolling of the applicator is along the longitudinal axis of the patient, while the pitching of the applicator occurs along the transversal axis. Because shockwaves propagate in the same direction independently of the yaw angle of the shockwave head, this angle is not relevant. Therefore, the implementation of a magnetometer was excluded. The accuracy of angle measurements was verified for angles ranging from 0 to $90°$. Negative angles were not included in the verification process because the positive range represents the negative range. This is due to the fact that obtaining the raw accelerometer and gyroscope data, as well as the subsequent angle estimation, operates identically for both positive and negative angles, differing only in sign. Angles from 90 to $180°$ and from -90 to $-180°$ were also excluded from the verification process because the angle displacement of the shockwave head within these ranges are not utilized in spinal cord shockwave therapy.

Initially, it was not clear if the prototype withstands the electromagnetic interference of the electrohydraulic shockwave head CSP0200 with a spark discharge of $25\,\mathrm{kV}$. Therefore, this test was conducted to evaluate how the measurement of the IMU data, and hence the angle estimation, was affected by the emitted shockwaves. The microcontroller of the prototype without any shielding had severe problems with the electromagnetic disturbances caused by the shockwave applicator CSP0200. The time interval of the timer interrupt switched from $4\,\mathrm{ms}$ to $30\,\mathrm{ms}$ after a couple of emitted shockwaves, adversely affecting the calculation of the angle displacement. To mitigate these disturbances, the prototype was wrapped in aluminum foil for improved electromagnetic compatibility (EMC). According to the illustration in Figure 3 and 4, the shockwaves induced peaks in the IMU data, where the amplitude depends on the distance between the shockwave head and the prototype. This observation supports the hypothesis that the peaks were caused by the shockwaves. Despite these peaks, the angle estimation was not influenced by the emitted shockwaves. This is due to the aspect that the accelerometer data are passed through a low-pass filter in the complementary filter, which effectively filters out rapid changes in the accelerometer data. Additionally, the peaks in the gyroscope data, reaching a maximum of $4\,\mathrm{s}^{-1}$, were low in comparison to the maximum values of approximately $150\,\mathrm{s}^{-1}$ in normal operation. The mean peak values, depicted in Table II, demonstrate that the peak values increase as the distance between the shockwave head and the prototype decreases. Especially in the gyroscope data, the difference in the distances is visible.

Despite the utilization of the aluminum foil, the external interrupt, which is triggered by the button under normal conditions to reset the orientation gets also triggered by the electromagnetic disturbances of the shockwave due to the oscillation. The input pin detects a rising edge, which triggers the external interrupt, even though it is configured with a pull-down or pull-up resistor. For future improvements of the prototype, EMC must be focused. Various strategies can be implemented to address this issue. One potential solution is to suspend the angle calculation during the emission of shockwaves. However, this approach does not resolve the timing issues of the microcontroller, and the compatibility test has shown that the IMU is not affected by the shockwaves. Connecting all unused pins of the microcontroller to a fixed potential, such as ground, can be a good option to combat the interference. This can reduce the potential for floating pins to pick up electromagnetic noise. Another option is to redesign the layout such that only the IMU and the visual indicators are placed inside the shockwave head and perform the angle calculation inside the high-voltage device. Consequently, the microcontroller is placed in an environment less susceptible to electromagnetic interference, improving the EMC performance of the system.

Although this paper demonstrates accurate angle measurement of a shockwave head in pitching and rolling, it has certain limitations. In the prototype setup, development boards for the microcontroller and the IMU were utilized to simplify programming via the onboard ST-LINK of the microcontroller. In future developments of the prototype, the development boards should be replaced with custom PCBs integrating the chips and their peripherals. To enhance usability for the physicians, it would be optimal to display the current angle displacement of the shockwave head on an OLED display or a similar device installed inside the shockwave head. For improved handling, the size of the electronics and the housing should be minimized.

Furthermore, a phantom test was not performed to verify that holding the shockwave head at the desired angle results in the maximum pressure pulse at the spinal cord. The hypothesis that applying shockwaves at $45°$ along the longitudinal axis yields the highest energy delivery, as currently practiced, was not confirmed [9]. Further investigations using a phantom model are necessary to determine if an angular displacement of the shockwave head in the transverse axis results in higher shockwave pressure at the lesion site.

No clinical trials or tests involving animals or humans were conducted in the course of this paper to demonstrate the efficacy of the real-time angle measurement system. Consequently, the system has not been verified in a medical setting yet. Future research should include clinical trials to evaluate the safety and efficacy of the system. Additionally,

feedback from medical professionals should be included in the transformation of the prototype into a serial product to ensure that it meets the user needs and expectations.

V. Conclusion

The sensor fusion of the IMU data was effectively integrated into the estimation of angular displacement of the shockwave head, thereby facilitating applicator alignment. Accuracy and precision of the angle calculation was proven. Additionally, the compatibility of the IMU with an electrohydraulic shockwave applicator has been demonstrated. Further development is needed to transform the prototype into a commercial product. Future research should include the evaluation of the prototype and future improvements within a clinical trial, demonstrating the safety and efficacy of real-time angle measurement during ESWT following SCI.

Acknowledgment

This paper was supported by the Management Center Innsbruck (MCI) and the company HeaRT Regeneration Technologies GmbH. I would like to express appreciation to both organizations for their valuable support and contributions to this research. Additionally, I extend my thanks to all participants and collaborators involved in this paper for their dedication and efforts.

References

[1] J. E. Bickenbach, Ed., *International perspectives on spinal cord injury*. Copenhagen: World Health Organization, European Observatory on Health Systems and Policies, op. 2013.

[2] K. Venkatesh, S. K. Ghosh, M. Mullick, G. Manivasagam, and D. Sen, "Spinal cord injury: pathophysiology, treatment strategies, associated challenges, and future implications," *Cell and Tissue Research*, vol. 377, pp. 125–151, 8 2019.

[3] K. Nas, L. Yazmalar, V. Şah, A. Aydın, and K. Öneş, "Rehabilitation of spinal cord injuries." *World journal of orthopedics*, vol. 6, pp. 8–16, 1 2015.

[4] C. Chaussy, W. Brendel, and E. Schmiedt, "Extracorporeally induced destruction of kidney stones by shock waves," *The Lancet*, vol. 316, pp. 1265–1268, 12 1980.

[5] M. Graber, F. Nägele, J. Hirsch, L. Pölzl, V. Schweiger, S. Lechner, M. Grimm, J. P. Cooke, C. Gollmann-Tepeköylü, and J. Holfeld, "Cardiac shockwave therapy - a novel therapy for ischemic cardiomyopathy?" *Frontiers in cardiovascular medicine*, vol. 9, p. 875965, 2022.

[6] V. Auersperg and K. Trieb, "Extracorporeal shock wave therapy: an update." *EFORT open reviews*, vol. 5, pp. 584–592, 10 2020.

[7] S. N. R. Alavi, A. M. Neishaboori, and M. Yousefifard, "Extracorporeal shockwave therapy in spinal cord injury, early to advance to clinical trials? a systematic review and meta-analysis on animal studies," *The Neuroradiology Journal*, vol. 34, pp. 552–561, 12 2021.

[8] M. Graber, F. Nägele, B. T. Röhrs, J. Hirsch, L. Pölzl, B. Moriggl, A. Mayr, F. Troger, E. Kirchmair, J. F. Wagner, M. Nowosielski, L. Mayer, J. Voelkl, I. Tancevski, D. Meyer, M. Grimm, M. Knoflach, J. Holfeld, and C. Gollmann-Tepeköylü, "Prevention of oxidative damage in spinal cord ischemia upon aortic surgery: First-in-human results of shock wave therapy prove safety and feasibility," *Journal of the American Heart Association*, vol. 11, 10 2022.

[9] I. Leister, R. Mittermayr, G. Mattiassich, L. Aigner, T. Haider, L. Machegger, H. Kindermann, A. Grazer-Horacek, J. Holfeld, and W. Schaden, "The effect of extracorporeal shock wave therapy in acute traumatic spinal cord injury on motor and sensory function within 6 months post-injury: a study protocol for a two-arm three-stage adaptive, prospective, multi-center, randomized, blinded, placebo-controlled clinical trial," *Trials*, vol. 23, p. 245, 12 2022.

[10] N. Reinhardt, C. Schmitz, S. Milz, and M. de la Fuente, "Influence of the skull bone and brain tissue on the sound field in transcranial extracorporeal shock wave therapy: an ex vivo study," *Biomedical Engineering / Biomedizinische Technik*, vol. 69, pp. 27–37, 2 2024.

[11] R. Beisteiner, E. Matt, C. Fan, H. Baldysiak, M. Schönfeld, T. P. Novak, A. Amini, T. Aslan, R. Reinecke, J. Lehrner, A. Weber, U. Reime, C. Goldenstedt, E. Marlinghaus, M. Hallett, and H. Lohse-Busch, "Transcranial pulse stimulation with ultrasound in alzheimer's disease—a new navigated focal brain therapy," *Advanced Science*, vol. 7, 2 2020.

[12] T. Popescu, C. Pernet, and R. Beisteiner, "Transcranial ultrasound pulse stimulation reduces cortical atrophy in alzheimer's patients: A follow-up study," *Alzheimer's & Dementia: Translational Research & Clinical Interventions*, vol. 7, 1 2021.

[13] P. Gui, L. Tang, and S. Mukhopadhyay, "Mems based imu for tilting measurement: Comparison of complementary and kalman filter based data fusion," *Proceedings of the 2015 10th IEEE Conference on Industrial Electronics and Applications, ICIEA 2015*, pp. 2004–2009, 11 2015.

[14] S. Colton and F. R. C. Mentor, "The balance filter," *Presentation, Massachusetts Institute of Technology*, 2007.

[15] "Towards understanding IMU: Basics of accelerometer and gyroscope sensors and how to compute pitch, roll and yaw angles - atadiat," accessed on 2024-06-24. [Online]. Available: https://atadiat.com/en/e-towards-understanding-imu-basics-of-accelerometer-and-gyroscope-sensors/

Alexander Plattner is with the Department of Medical and Health Technologies, MCI, Innsbruck, Austria. Among others he is responsible for the activities in medical engineering in which he is regularly publishing.